Extremophiles (2001) 5:323–332
Digital Object Identifier (DOI) 10.1007/s007920100208

ORIGINAL PAPER

Servé W.M. Kengen · Floris J. Bikker · Wilfred R. Hagen
Willem M. de Vos · John van der Oost

Characterization of a catalase-peroxidase from the hyperthermophilic archaeon *Archaeoglobus fulgidus*

Received: January 30, 2001 / Accepted: April 5, 2001 / Published online: August 17, 2001

Abstract A putative *perA* gene from *Archaeoglobus fulgidus* was cloned and expressed in *Escherichia coli* BL21(DE3), and the recombinant catalase-peroxidase was purified to homogeneity. The enzyme is a homodimer with a subunit molecular mass of 85 kDa. UV–visible spectroscopic analysis indicated the presence of protoheme IX as a prosthetic group (ferric heme), in a stoichiometry of 0.25 heme per subunit. Electron paramagnetic resonance analysis confirmed the presence of ferric heme and identified the proximal axial ligand as a histidine. The enzyme showed both catalase and peroxidase activity with pH optima of 6.0 and 4.5, respectively. Optimal temperatures of 70°C and 80°C were found for the catalase and peroxidase activity, respectively. The catalase activity strongly exceeded the peroxidase activity, with V_{max} values of 9600 and 36 U mg^{-1}, respectively. K_m values for H_2O_2 of 8.6 and 0.85 mM were found for catalase and peroxidase, respectively. Common heme inhibitors such as cyanide, azide, and hydroxylamine inhibited peroxidase activity. However, unlike all other catalase-peroxidases, the enzyme was also inhibited by 3-amino-1,2,4-triazole. Although the enzyme exhibited a high thermostability, rapid inactivation occurred in the presence of H_2O_2, with half-life values of less than 1 min. This is the first catalase-peroxidase characterized from a hyperthermophilic microorganism.

Key words Catalase · Peroxidase · *Archaeoglobus* · Hyperthermophile · Heme

Communicated by G. Antranikian

S.W.M. Kengen (✉) · F.J. Bikker · W.R. Hagen · W.M. de Vos · J. van der Oost
Laboratory of Microbiology, Department of Agrotechnology and Food Sciences, Wageningen University, Hesselink van Suchtelenweg 4, NL-6703 CT Wageningen, The Netherlands
Tel. +31-317-483748; Fax +31-317-483829
e-mail: serve.kengen@algemeen.micr.wag-ur.nl

Presented at the Third International Congress on Extremophiles, Hamburg, 2000

Introduction

Archaeoglobus fulgidus is a strict anaerobic hyperthermophilic archaeon that has been isolated from marine hydrothermal environments as well as subsurface oil fields. This sulfate reducer can grow organoheterotrophically with a variety of carbon sources, or lithoautotrophically on hydrogen, thiosulfate, and CO_2 (Stetter 1988). Besides its ability to grow at extremely high temperatures, this organism is unusual in that it is unrelated to other sulfate reducers.

Recently, the sequencing of the entire genome of *A. fulgidus* was completed (Klenk et al. 1997). The sequencing revealed the presence of an open reading frame that was putatively identified as a catalase-peroxidase on the basis of its high similarity (62.9% nucleotide identity; 49.5% amino acid similarity) to the *perA* gene of *Bacillus stearothermophilus* (Klenk et al. 1997; Loprasert et al. 1989). The *Bacillus* enzyme belongs to the group of so-called bacterial catalase-peroxidases, which exhibit substantial catalase ($H_2O_2 \rightarrow H_2O + 1/2O_2$) as well as peroxidase activity ($AH_2 + H_2O_2 \rightarrow A + 2H_2O$) (Welinder 1991, 1992). Despite the often high catalase activity of this group of heme-containing enzymes, they are not related to the monofunctional catalases. On the basis of sequence similarity, the catalase-peroxidases are grouped in class I of the superfamily of plant, fungal, and bacterial peroxidases (Welinder 1992). Class II consists of secretory fungal peroxidases (ligninases and manganese-peroxidases). Class III is the secretory plant peroxidases, including horseradish peroxidase.

In recent years, various catalase-peroxidases have been purified and characterized, and their genes have been sequenced (Brown-Peterson and Salin 1993; Cendrin et al. 1994; Fraaije et al. 1996; Hochman and Shemesh 1987; Loprasert et al. 1988; Levy et al. 1992; Marcinkeviciene et al. 1995; Morris et al. 1992; Mutsuda et al. 1996; Obinger et al. 1997; Regelsberger et al. 1999; Triggs-Raine et al. 1988). In contrast to the monomeric peroxidases from plants, fungi, and yeasts, the bacterial catalase-peroxidases are dimers or tetramers. The subunit size of the bacterial catalase-peroxidases (approximately 80 kDa) is about twice

the size of the monomeric peroxidases (33–40 kDa). Typical catalases differ from the catalase-peroxidases and other peroxidases in that the ferric heme is not reducible by dithionite, and that the enzyme can be inhibited by 3-amino-1,2,4-triazole (Nadler et al. 1986). Moreover, in contrast to peroxidases, catalases show a broad optimal pH range (Nadler et al. 1986).

Besides true "bacterial" catalase-peroxidases, class I also contains eukaryal and archaeal representatives, viz., the catalase-peroxidases from the fungi *Penicillium simplicissimum* (Fraaije et al. 1996) and *Septoria tritici* (Levy et al. 1992), as well as from the extreme halophiles *Halobacterium salinarum* (Brown-Peterson and Salin 1993) and *Haloarcula marismortui* (Cendrin et al. 1994). For the fungal enzymes, the classification in the catalase-peroxidase group is based on their biochemical properties only, because sequence data are not yet available.

We here present a characterization of the putative *perA* gene product of *A. fulgidus*. On the basis of its primary structure, it probably also belongs to the group of bacterial catalase-peroxidases, and it would represent the first catalase-peroxidase from a hyperthermophilic microorganism. Enzymes from (hyper)thermophiles generally exhibit a high stability with respect to temperature, but also towards chemical denaturants, such as detergents or organic solvents (Jaenicke 1991; Leuschner and Antranikian 1995). Such increased stability may be advantageous for the application of the enzyme. In order to analyze its biochemical properties and to test its potential stability, the *perA* gene was cloned and expressed in *Escherichia coli*, and the overproduced catalase-peroxidase was purified and compared with other catalase-peroxidases.

Materials and methods

Materials

2,2′ - Azino - bis(3 - ethylbenzthiazoline - 6 - sulfonic acid) (ABTS), 3,3′-dimethoxybenzidine, and 4-aminoantipyrine were obtained from Sigma Chemie (Bornem, Belgium). *p*-Phenylenediamine and 3-amino-1,2,4-triazole were from J.T. Baker Chemicals (Deventer, The Netherlands). 2,4 Dichlorophenol and 3,3′-diaminobenzidine were obtained from Acros (Beerse, Belgium). The Q-Sepharose, Superdex 200 HR 10/30, and Mono-Q HR 5/5 columns were from Amersham Pharmacia Biotech (Woerden, The Netherlands). Hydroxyapatite (Bio-Gel HT) and sodium dodecyl sulfate-polyacrylamide gel electrophoresis (SDS-PAGE) calibration proteins (broad range) were purchased from Bio-Rad (Veenendaal, The Netherlands). The pET9d expression vector was obtained from Novogen (Madison, WI, USA). *E. coli* BL21(DE3) and *Pfu* DNA polymerase were from Stratagene (La Jolla, CA, USA). *Archaeoglobus fulgidus* (DSM 4304) was obtained from the German Collection of Microorganisms and Cell Cultures (Braunschweig, Germany).

Cloning of the catalase-peroxidase gene

In the genome sequence of *A. fulgidus* (Klenk et al. 1997), a putative catalase-peroxidase gene (*perA*; AF2233) was identified with 62.9% identity to the *perA* gene of catalase I of *Bacillus stearothermophilus* (M29876). The following primer set was designed to amplify the open reading frame by polymerase chain reaction (PCR): BG597 (5′-gcgcg**ccatg g**atgatgagacagggtggtgttatg, sense) and BG599 (5′-cgcgc**gg atcc**tcacctcaaacctgcggttatctc, antisense), with *Nco*I and *Bam*HI restriction sites in bold. The 50-µl PCR reaction mixture contained 200 ng *A. fulgidus* SL-5 genomic DNA, isolated as described by Sambrook et al. (1989), 50 ng of each primer BG597 and BG599, 0.2 mM dNTPs, *Pfu* polymerase buffer, and 2.5 units *Pfu* DNA polymerase, and was subjected to 30 cycles of amplification (1 min at 94°C, 1 min at 60°C, and 2 min at 72°C) on a DNA thermal cycler (Perkin-Elmer Cetus, Norwalk, CT, USA). The PCR product was digested (*Nco*I/*Bam*HI) and cloned into an *Nco*I/*Bam*HI-digested pET9d vector, resulting in pLUW640, which was transformed into *E. coli* BL21(DE3) by heat shock. Sequence analysis on pLUW640 was done by the dideoxynucleotide chain termination method with a Li-Cor automatic sequencing system (model 4000L; Lincoln, NE, USA). Sequencing data were analyzed using DNAStar software (London, England).

Overexpression of the catalase-peroxidase gene in *E. coli*

An overnight culture of *E. coli* BL21(DE3) containing pLUW640 was used as a 1% inoculum in 2 l LB medium with 50 µg/ml kanamycin. After growth for 15 h at 37°C, cells (8.6 g wet weight) were harvested by centrifugation (2200*g* for 20 min) and resuspended in 27 ml 50 mM Tris/HCl buffer, pH 7.8. The suspension was passed through a French press (110 MPa), and the resulting crude cell extract was used for purification of the recombinant catalase-peroxidase.

Purification of the recombinant catalase-peroxidase

The *E. coli* cell extract was heated for 30 min at 80°C, and denatured proteins were pelleted by centrifugation (17,200 *g* for 20 min). This pellet fraction was washed with 10 ml of buffer, and the centrifugation step was repeated. The supernatants of both centrifugation steps were combined, filtered through a 0.45-µm filter and loaded onto a Q-Sepharose column (1.6 × 10 cm) that was equilibrated with 20 mM Tris/HCl buffer (pH 7.8). Bound proteins were eluted by a 300-ml linear gradient of NaCl (0 to 1 M in Tris/HCl buffer). The catalase-peroxidase eluted in a single peak at 0.2 M NaCl. Active fractions were pooled and applied to a hydroxyapatite column (Bio-Gel HT; 2.6 × 12 cm) equilibrated with 10 mM sodium phosphate buffer (pH 7.0). Elution was performed with a 500-ml gradient from 10 to 500 mM sodium phosphate (pH 7.0). The catalase-peroxidase eluted at approximately 0.1 M sodium

phosphate. Active fractions were pooled and concentrated by ultrafiltration (Filtron Technology, Northborough, MA, USA; 30 kDa cutoff). The concentrated sample was loaded in 500-µl aliquots onto a Superdex-200 HR column, equilibrated in 20 mM Tris/HCl (pH 7.8) containing 100 mM NaCl. The active pools were combined, diluted with an equal volume of demineralized water, and loaded onto a Mono-Q HR 5/5 column equilibrated in 20 mM Tris/HCl (pH 8.0). The catalase-peroxidase eluted at 0.075 M NaCl during a 30-ml linear NaCl gradient (0 to 0.5 M). Fractions that gave a single band on a native PAGE gel were pooled.

Polyacrylamide gel electrophoresis

The purity of the various purification fractions was regularly checked by sodium dodecyl sulfate-polyacrylamide gel electrophoresis (SDS-PAGE) or native PAGE, according to the procedure of Laemmli using 10% (w/v) gels (Laemmli 1970). Protein samples were denatured by heating in SDS sample buffer for 5 min at 100°C. SDS-PAGE was also used to determine the subunit molecular mass. Calibration was performed using a set of calibration proteins: myosin (200 kDa), β-galactosidase (116.25 kDa), phosphorylase b (97.4 kDa), serum albumin (66.2 kDa), ovalbumin (45 kDa), and carbonic anhydrase (31 kDa). Protein bands were stained with Coomassie brilliant blue R250.

Enzyme assays

Peroxidase and catalase activity was measured spectrophotometrically in 1-ml quartz cuvettes on a Hitachi U-2010 spectrophotometer (Hitachi Science Systems, Hitachinaka, Japan) equipped with a thermostatted cuvette holder. Peroxidase activity was determined by monitoring the oxidation of ABTS by H_2O_2 at 405 nm and at 70°C ($\in_{405}$ = 36.8 $mM^{-1}\,cm^{-1}$). The standard assay mixture (1 ml) contained potassium phosphate/sodium citrate buffer (50 mM each; pH 4.5), 0.9 mM ABTS, 15 mM H_2O_2, and an appropriate amount of enzyme. Because of the relatively high catalase activity, care was taken that during the assay the H_2O_2 concentration remained far above the K_m. Therefore, the initial rates were calculated from the absorbance change in the first seconds of the reaction. Due to the stabilizing effect of ABTS (vide infra), the assay was not disturbed by the inactivation of the enzyme in the presence of H_2O_2. The assay gave a linear relationship between the amount of enzyme added (0.1–3.2 µg protein) and the activity (not shown). 3,3′-Dimethoxybenzidine ($\in_{460}$ = 11.3 $mM^{-1}\,cm^{-1}$), 3,3′-diaminobenzidine, 4-aminoantipyrine/2,4 dichlorophenol ($\in_{500}$ = 1.36 $mM^{-1}\,cm^{-1}$), *p*-phenylenediamine, nicotinamide adenine dinucleotide, reduced (NADH), and nicotinamide adenine dinucleotide phosphate, reduced (NADPH) ($\in_{340}$ = 6.2 $mM^{-1}\,cm^{-1}$) were tested as alternative electron donors instead of ABTS. Catalase activity was determined by monitoring the decrease of H_2O_2 at 240 nm ($\in_{240}$ = 43.6 $M^{-1}\,cm^{-1}$). The standard assay mixture (1 ml) contained potassium phosphate/sodium citrate buffer (50 mM each; pH 6.0), 30 mM H_2O_2, and an appropriate amount of enzyme. Specific activities were calculated from the initial linear change in absorbance. There was no non-enzymatic disproportionation of H_2O_2 observed at 70°C. The catalase assay showed a linear relationship between the amount of enzyme (0.58–4.65 µg protein) and the activity (not shown). For estimating the effect of ABTS on the catalase activity, an alternative catalase assay was used in which the release of oxygen was measured polarographically with a Clark-type oxygen electrode (Yellow Springs Instruments, Yellow Springs, OH, USA). The reaction mixture consisted of 3 ml phosphate/citrate buffer (pH 4.5), 10 mM H_2O_2, and 0.9 mM ABTS. The reaction was performed at 50°C, and was started by the addition of an appropriate amount of enzyme. One unit (U) is defined as the amount of enzyme that catalyzes the conversion of 1 µmol of H_2O_2 per min. The activity of compounds for which no absorbance coefficient has been reported (3,3′-diaminobenzidine, *p*-phenylenediamine) was expressed as absorbance units per min (AU min^{-1}).

Protein was determined according to Bradford (1976) using the BioRad protein assay kit, with bovine serum albumin as a standard.

Spectroscopic analysis

The UV–visible spectra were recorded on a Hitachi U-2010 spectrophotometer at 20°C. For the "as isolated" spectrum, purified enzyme was diluted in phosphate/citrate buffer (50 mM each, pH 7.0) to 0.25 mg/ml. Subsequently, KCN was added to a concentration of 10 mM. The reduced spectrum was obtained through the addition of sodium dithionite (~0.4 mM) to a similar enzyme solution, which was flushed with N_2 gas in a stoppered cuvette. The pyridine hemochrome spectrum ($\in_{418}$ = 191.5 $mM^{-1}\,cm^{-1}$) was obtained after reduction with dithionite in 20% (w/v) pyridine and 0.1 M NaOH.

Electron paramagnetic resonance spectroscopy

Electron paramagnetic resonance (EPR) spectra were recorded on a Bruker ER-200 D spectrometer (Bruker Instruments, Billerica, MA, USA) and simulated using equipment and software as described by Schumacher et al. (1997) and references therein.

Analysis of catalytic properties

Kinetic parameters were determined for the catalase and peroxidase reaction by using the standard assay systems at 70°C. The concentration of H_2O_2 was varied between 0.1 and 2.5 mM and between 1.5 and 30 mM for the peroxidase and catalase activity, respectively. Kinetic data were obtained by a computer-aided direct fit to the Michaelis-Menten curve. The temperature dependence of the catalase and peroxidase activity was determined in the range from

20°C to 90°C. The pH-dependence was determined in the standard potassium phosphate/sodium citrate buffer at 70°C.

Stability analysis

The thermostability of the enzyme was tested by incubating the purified enzyme (0.24 mg/ml) in Tris/HCl buffer (pH 7.8) in a closed vial in a water bath at 70°C for 400 min. At regular time intervals, a sample was taken and tested using the standard assay. The stability in the presence of H_2O_2 was determined by adding the enzyme to the standard assay mixture at 70°C in the presence of different amounts of H_2O_2, but in the absence ABTS. After 15, 30, 45, and 60 s of preincubation, the reaction was started by the addition of ABTS. The stabilizing effect of ABTS on the inactivation by H_2O_2 was determined by following the catalase activity (oxygen formation) in the presence and absence of ABTS as described earlier.

Results

Cloning and expression

The *perA* gene from *A. fulgidus* was successfully cloned into *E. coli* BL21 (DE3) using the pET9d vector system, as confirmed by sequence analysis of pLUW640 (not shown). Active catalase-peroxidase was demonstrated in the *E. coli* extract and amounted to approximately 2% of the total protein content.

Purification of the recombinant enzyme

Due to their high thermostability, enzymes from hyperthermophiles are generally rather easily purified from a cell extract of a mesophilic host. Also in this case, a heat treatment resulted in the removal of the majority of contaminating *E. coli* proteins (Fig. 1). Nevertheless, four subsequent chromatographic steps were necessary to obtain a homogeneous preparation (Table 1). The SDS-PAGE pattern (Fig. 1A) was rather misleading in this respect; three major bands were visible in all steps. However, analysis on a native gel showed a single band in the final preparation, suggesting that these three bands apparently represented different forms of the catalase-peroxidase (Fig. 1B). The three bands obtained after SDS-PAGE corresponded to molecular masses of 87, 82, and 54 kDa. From the derived amino acid sequence, a molecular mass of 84.9 kDa was calculated for the apoenzyme, which is in the same range as the upper two bands on the gel. Gel filtration on the Superdex 200 indicated a molecular mass of the native enzyme of 169 kDa, which suggests that the catalase-peroxidase is a homodimer. As expected, comparable purification factors (~3-fold) as well as recoveries (~32%) were obtained for the catalase and the peroxidase activity (Table 1).

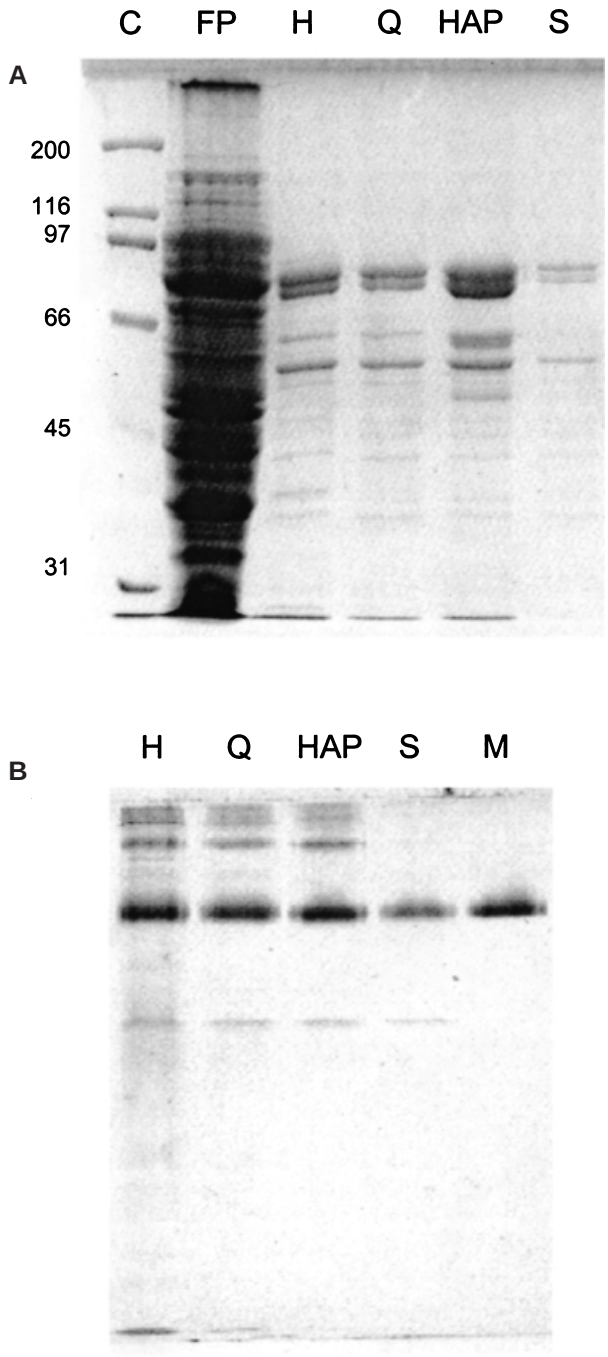

Fig. 1. Sodium dodecyl sulfate-polyacrylamide gel electrophoresis (SDS-PAGE) (**A**) and native PAGE (**B**) of various samples of catalase-peroxidase from *A. fulgidus*. *C*, calibration proteins; *FP*, cell extract after French press; *H*, supernatant of heat-treated extract; *Q*, Q-Sepharose fraction; HAP, hydroxyapatite fraction; S, Superdex 200 fraction; M, Mono-Q fractions 27–31. The molecular mass of the calibration proteins is indicated (kDa). Amount of protein loaded on gel: (**A**) *FP*, 199 µg; *H*, 14.5 µg; *Q*, 5 µg; *HAP*, 10 µg; *S*, 1.2 µg. (**B**) *H*, 14.5 µg; *Q*, 5 µg; *HAP*, 5 µg; *S*, 2.4 µg; *M*, 4.9 µg

Catalytic properties

For the assay of peroxidases, various organic electron donors can be used. 3,3′-Dimethoxybenzidine (4.6 U mg^{-1}), 3,3′-diaminobenzidine (114 AU min^{-1} mg^{-1}), *p*-phenylenedi-

Table 1. Purification scheme of the catalase-peroxidase from *A. fulgidus*. Both catalase and peroxidase activities are shown

	Total volume ml	Protein mg/ml	Total protein mg	Catalase				Peroxidase			
				Specific activity U/mg	Total activity U	Purification -fold	Recovery %	Specific activity U/mg	Total activity U	Purification -fold	Recovery %
Crude extract	23.75	39.8	946	–	–	–	–	0.45	425	–	–
Heat-treatment	33.68	2.91	98.0	2375	232 724	1	100	7.4	722	1	100
Q-sepharose	42.80	1.01	43.4	3964	172 058	1.67	74	13.3	575	1.80	80
Hydroxyapatite	16.52	2.02	33.4	5542	185 105	2.33	79	18.3	614	2.49	85
Superdex 200	75.72	0.24	17.9	6817	122 018	2.87	52	22.1	397	3.00	55
Mono-Q (27–31)	17.35	0.61	10.6	6922	73 377	2.91	31	23.3	247	3.17	34

amine (121 AU min^{-1} mg^{-1}), and aminoantipyrine together with 2,4-dichlorophenol (5.2 U mg^{-1}) showed significant peroxidase activity. Because of its high absorption coefficient and good solubility in water, ABTS was the preferred substrate for routine measurements. No activity was detected with NADH or NADPH.

In the presence of H_2O_2, the enzyme rapidly inactivated. At a H_2O_2 concentration of 1 mM, a half-life of inactivation of approximately 60 s was found. At lower temperatures, the rate of inactivation was less, but half-lifes were still in the range of a few minutes. ABTS was able to diminish the inactivation by H_2O_2. This effect was observed best by measuring catalase activity in the presence and absence of ABTS. In the absence of ABTS, the catalase activity decreased with a half-life of approximately 20 s, whereas in the presence of ABTS, the rate of inactivation was about threefold lower. Because peroxidase activities were determined in the first seconds of the reaction, the assay was not disturbed by the rapid inactivation of the enzyme in the presence of H_2O_2. Moreover, ABTS protected the enzyme from inactivation by H_2O_2. However, the quantification of the catalase activity may have been influenced by the inactivation by H_2O_2. Because of the relatively low extinction coefficient (43.6 M^{-1} cm^{-1}), the initial rate determination was not possible within a few seconds. Moreover, ABTS was not present in these assays and thus could not exert its stabilizing effect. For these reasons, the values for the catalase are probably underestimated, but they are the best achievable.

In accordance with the physiological growth optimum of *A. fulgidus* of 83°C, the catalase-peroxidase exhibited high thermostability. Incubation of the enzyme at 70°C for 400 min did not result in a significant decrease in activity (not shown).

The optimum pH for the peroxidase and catalase activity was 4.5 and 6, respectively (Fig. 2A). The optimum temperature for the peroxidase was found at 80°C, corresponding to the physiological growth optimum of the organism (Fig. 2B). The increase in peroxidase activity followed a linear Arrhenius plot (ln *k* versus 1/T; not shown), from which an activation energy of 37.1 kJ mol^{-1} could be calculated. The temperature-dependence of the catalase activity, however, did not obey the Arrhenius's theory, suggesting that the activity at higher temperatures is probably underestimated.

Table 2. Effect of inhibitors on the catalase and peroxidase activity of the catalase-peroxidase of *A. fulgidus*

Inhibitor	Inhibitor concentration (mM) required for 50% inhibition	
	Catalase	Peroxidase
3-Amino-1,2,4-triazole	6	30
Hydroxylamine	0.02	1.5
Sodium azide	0.025	0.15
Potassium cyanide	1	1

The catalase-peroxidase was inhibited by potassium cyanide, sodium azide, and hydroxylamine, which are all typical inhibitors of heme enzymes (Table 2). However, much higher concentrations of hydroxylamine and sodium azide were required to inhibit the peroxidase activity than the catalase activity. Also, unlike in the case of other catalase-peroxidases, 3-amino-1,2,4-triazole, an inhibitor of monofunctional catalases, inhibited the catalase as well as the peroxidase activity.

The apparent K_m and V_{max} values of the peroxidase activity was 0.85 ± 0.13 mM, and 35.9 ± 2.2 U mg^{-1}, respectively. These values are in the same range as those found for several other catalase-peroxidases, which are between 0.1 and 1.3 mM for K_m and between 0.8 and 105 U mg^{-1} for V_{max}. The catalase activity also showed Michaelis-Menten–like kinetics, which resulted in K_m and V_{max} values of 8.6 ± 1.2 mM and 9600 ± 550 U mg^{-1}, respectively. However, as has been discussed by Hochman and Shemesh (1987), the rate of catalase activity should increase linearly with the H_2O_2 concentration, and it is, therefore, incorrect to treat the catalase kinetics as conforming to Michaelis-Menten kinetics. The apparent saturation observed for the catalase activity could be a result of the inhibitory effect of H_2O_2, which increases at higher H_2O_2 concentrations.

Spectral properties

The UV–visible spectra of the "as isolated" catalase-peroxidase showed typical high-spin ferric heme features with a maximum at 403 nm and shoulders at 500 and 630 nm

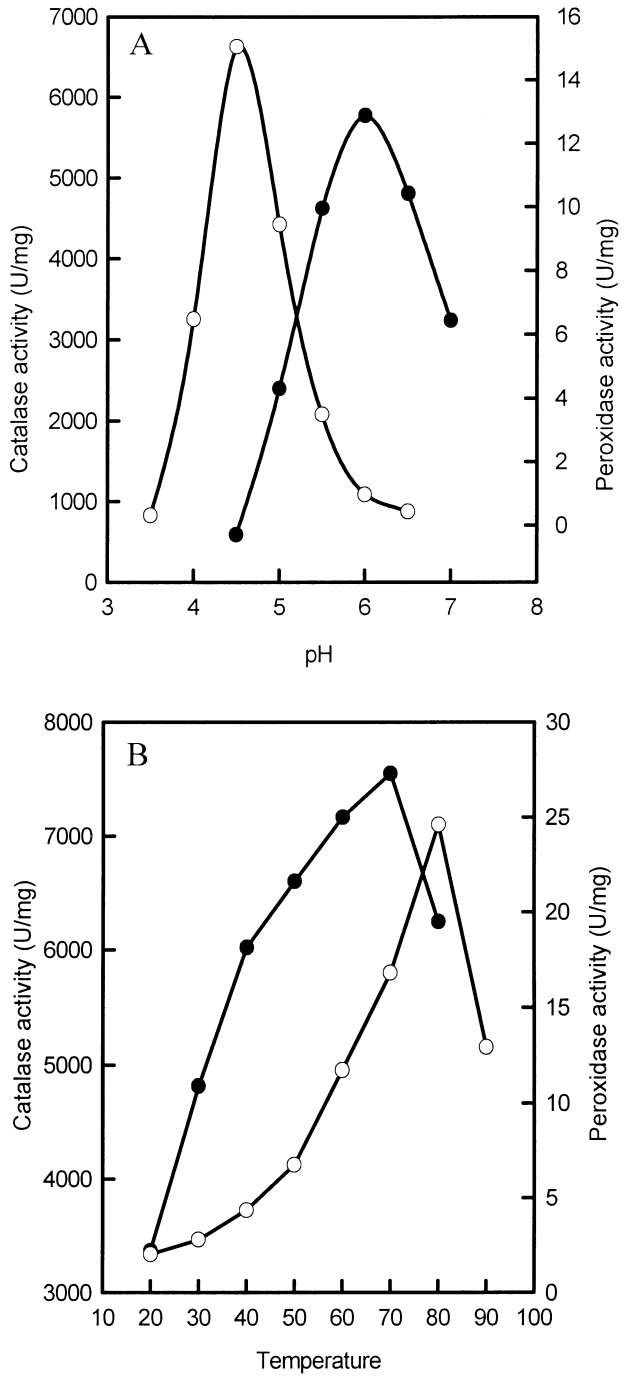

Fig. 2. pH dependence (**A**) and temperature dependence (**B**) of the catalase (*solid circles*) and peroxidase (*open circles*) activity

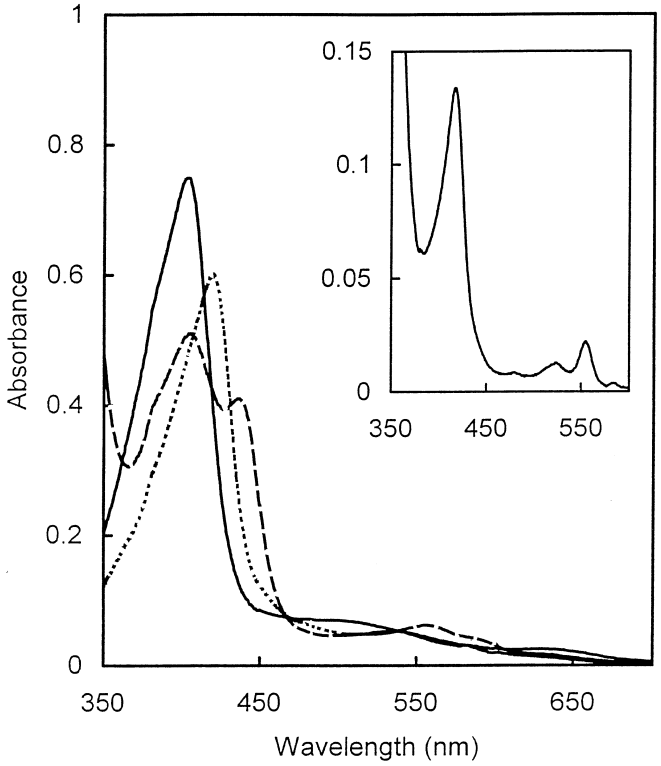

Fig. 3. UV–Visible absorbance spectrum of the catalase-peroxidase of *A. fulgidus*. As isolated (*solid line*); after reduction with dithionite (*dashed line*); after addition of KCN (*dotted line*). The *inset* shows the pyridine hemochrome spectrum

(Fig. 3). An *RZ* ratio ($A_{(\text{Soret peak})}/A_{280}$) of 0.32 was found for the purified enzyme. Addition of cyanide to the oxidized enzyme resulted in a shift of the Soret band to 415 nm. Reduction of the enzyme with dithionite caused the Soret band to decrease and to shift to 438 nm, with a new maximum appearing at 556 nm. The pyridine hemochrome spectrum was obtained after reduction with dithionite in pyridine/NaOH (Fig. 3, inset). The spectrum is identical to that of protoheme IX, with α- and β-bands at 555 and 524 nm, respectively, and the Soret peak at 417. From the maximum at 417 nm, a heme content of 0.25 heme per subunit could be calculated.

The low-temperature EPR spectrum of the catalase-peroxidase "as isolated" is characteristic of a high-spin ferric heme with features around $g = 6$ and 2 (Fig. 4). The feature around $g = 6$ consists of several pairs of lines, indicating that the iron environment in the heme occurs in several forms of slightly different rhombicity. Such a microscopic "heterogeneity" is quite common for hemoproteins (Hartzell and Beinert 1974; Pierik and Hagen 1991), but its biological relevance has not been established. Analysis by simulation of high-spin ferric heme spectra is difficult, because the line width is determined by the convoluted effects of distributions in zero-field splittings, *g*-strain, and unresolved superhyperfine splittings (Hagen 1981). In Fig. 4, a simulation based on *g*-strain broadening only is included in order to estimate the number and relative intensity of the forms with different rhombicity. At least four different forms are required in order to obtain a reasonable simulation (fit parameters not shown). The very weak peak at $g = 3.12$ is the low-field peak of a low-spin ferric heme. The concentration of this low-spin derivative is estimated, by *g*-strain simulation, to be approximately 3% that of the combined high-spin components. Reduction of the enzyme with sodium dithionite in the presence of excess sodium nitrite yields the low-spin ferrous heme form complexed with nitric oxide, NO, in the sixth axial ligand position. The unpaired electron of the NO delocalizes via the Fe to the fifth axial ligand. If this ligand happens to be a nitrogen from a histidyl

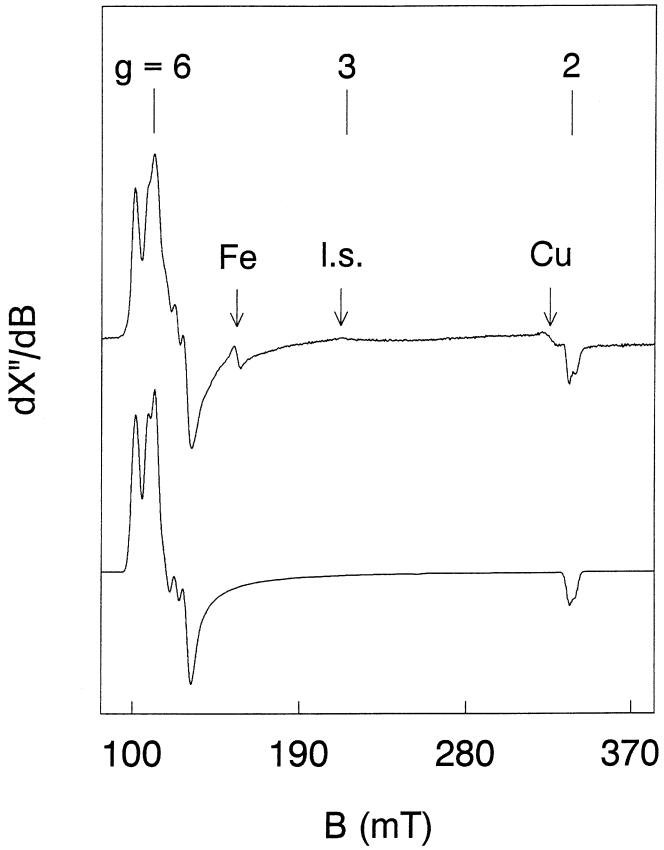

Fig. 4. Electron paramagnetic resonance (EPR)-spectrum (*upper trace*) and simulation (*lower trace*) of the Fe(III) heme in *A. fulgidus* catalase-peroxidase. The enzyme preparation contained 23.5 mg protein ml^{-1} (140 µM dimeric protein) in 20 mM Tris/HCl buffer (pH 8.0) with 75 mM NaCl. The spectrum is dominated by four forms of high-spin ferric heme. A weak peak at $g_z = 3.12$ is from approximately 3% low-spin (*l.s.*) heme (g = 3.12, 2.2, 1.3). Other features from minor (<1%) contaminants of non-heme iron (*Fe*) and of copper (*Cu*) are indicated with *arrows*. EPR conditions: microwave frequency, 9407 MHz; microwave power, 8 mW; modulation frequency, 100 kHz; modulation amplitude, 0.63 mT; temperature, 10.5 K

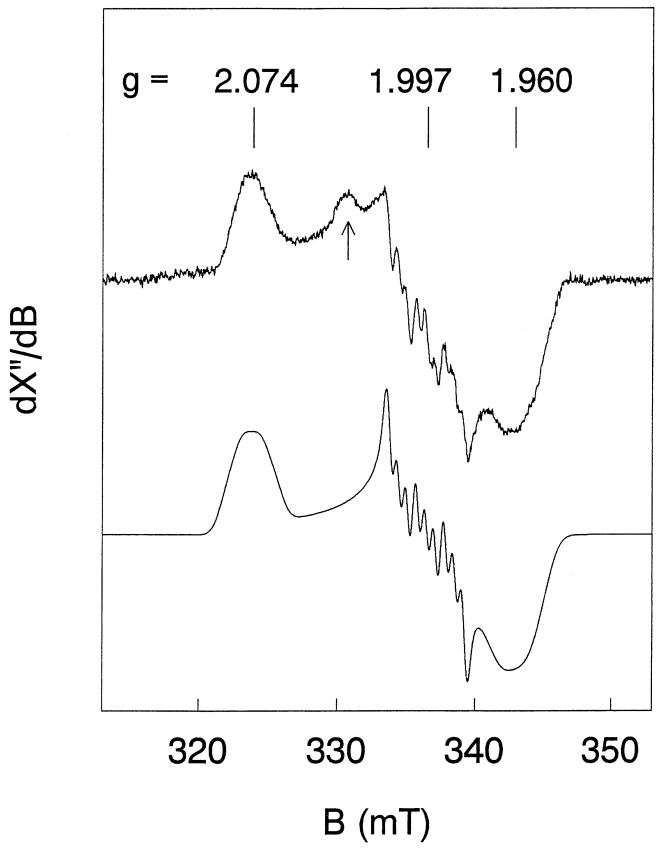

Fig. 5. EPR spectrum (*upper trace*) and simulation (*lower trace*) of the NO derivative of Fe(II)heme in *A. fulgidus* catalase-peroxidase. The enzyme of Fig. 5 was incubated with 50 mM sodium nitrite and, subsequently, for 10 min with 5 mM buffered sodium dithionite. The spectrum exhibits the characteristic splitting pattern from one dominant nitrogen (NO) and one weaker nitrogen (His), which proved the fifth ligand to the Fe to be histidine. A minor signal indicated by an *arrow* is the result of excess free NO radical. EPR conditions: microwave frequency, 9406 MHz; microwave power, 0.2 mW; modulation frequency, 100 kHz; modulation amplitude, 0.13 mT; temperature, 23 K

residue, the resulting EPR spectrum exhibits not only hyperfine splitting from the ^{14}N (I = 1) nucleus of NO, but also, although weaker, from the coordinating histidyl-N (Yonetani et al. 1972). In Fig. 5, the EPR spectrum of Fe(II)NO catalase-peroxidase is presented. The "triplet-of-triplets" pattern of nine lines is clearly visible, and this interpretation is further corroborated by spectral simulation. Hence, it is concluded that the fifth ligand to the heme Fe in *A. fulgidus* catalase-peroxidase is a histidine.

Amino acid sequence analysis

Multiple sequence alignment of the *A. fulgidus* PerA enzyme and several bacterial and archaeal catalase-peroxidases showed a high overall similarity (47.5% to 70.0%; see legends of Fig. 6 for accession numbers). The putative active site residues present in all catalase-peroxidases could also be identified in the *A. fulgidus* sequence, i.e., His-249 presumably acts as the proximal axial ligand of the heme iron and His-87, Trp-86, and Arg-83 are probably the conserved residues at the distal side of the heme that form the ligand pocket for H_2O_2.

An evolutionary tree of several bacterial catalase-peroxidases, with a horseradish peroxidase isozyme as outgroup, clearly shows the overall similarity of the bacterial catalase-peroxidases (Fig. 6).

Discussion

The *perA* gene from the hyperthermophilic archaeon *A. fulgidus* was successfully cloned and expressed in *E. coli*. The catalytic properties of the catalase-peroxidase produced resembled those of known bacterial enzymes, which is supported by the significant sequence similarity of the *A. fulgidus* enzyme to the so-called bacterial catalase-peroxidases. Although there are two other archaeal exam-

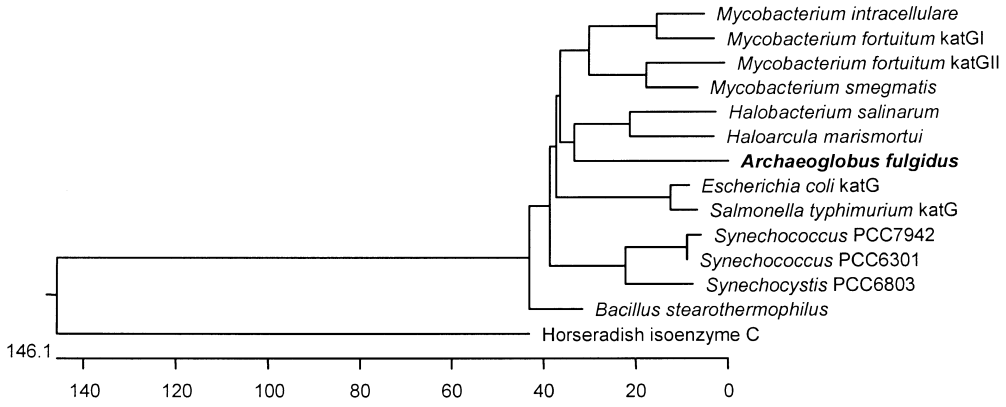

Fig. 6. Phylogenetic tree of catalase-peroxidases deduced from a comparison of their primary structures. A typical peroxidase (horseradish) was used as outgroup. The tree was constructed from alignments using the Clustal method of the Megalign program (DNAStar, London, England). The units at the bottom indicate the number of substitution events. Accession numbers: *Mycobacterium intracellulare*, M86741; *Mycobacterium fortuitum* katGI, Y07865; *Escherichia coli* katG, M21516; *Salmonella typhimurium* katG, X53001; *Halobacterium salinarum*, AF069761; *Haloarcula marismortui*, Y16851; *Archaeoglobus fulgidus*, AF2233; *Synechococcus* PCC7942, D61378; *Synochococcus* PCC6301, AF197161; *Synechocystis* PCC6803, D83990; *Bacillus stearothermophilus*, M29876; *Mycobacterium fortuitum* katGII, Y07866; *Mycobacterium smegmatis*, X98718; horseradish isoenzyme C, M6072

ples known, viz., the enzymes from *H. halobium* and from *H. marismortui*, the *A. fulgidus* enzyme represents the first catalase-peroxidase from a hyperthermophilic archaeon.

Based on the native molecular mass of 169 kDa and the subunit mass of 84.9 kDa, we conclude that the enzyme is a homodimer. This is comparable to other catalase-peroxidases, which are either dimers or tetramers of about 80 kDa.

The *A. fulgidus* enzyme showed both catalase and peroxidase activity, with apparent V_{max} values of 9600 U mg^{-1} and 35.9 U mg^{-1}, respectively. If we use the experimentally determined heme content (0.25 heme subunit^{-1}), k_{cat} values of 61.6×10^3 sec^{-1} and 230 sec^{-1} can be calculated for the catalase and peroxidase, respectively. The turnover number of the catalase is the highest of any catalase-peroxidases reported to date, especially if one considers that the value is probably underestimated. This also results in an extraordinarily high catalase/peroxidase ratio. At 70°C, the catalase activity is about 450-fold higher than the peroxidase activity, and at 20°C this ratio even amounts to 1700. For comparison, the enzymes from *H. salinarum* and *B. stearothermophilus* show catalase/peroxidase ratios of only 0.414 and 48, respectively (Brown-Peterson and Salin 1993; Loprasert et al. 1988). In this respect, the *A. fulgidus* enzyme resembles more the typical catalases. This is also reflected by the inhibition by amino-1,2,4-triazole, which has not been observed before for other catalase-peroxidases. These differences may be explained through the generally accepted catalytic mechanism, which involves several different iron oxo species of the heme (Fig. 7). Catalase-peroxidases exhibit much lower steady-state concentrations of compound I than monofunctional catalases, which have much higher apparent saturation constants (Hochman and Shemesh 1987). This difference in steady-state concentrations of compound I between catalase-peroxidases and typical catalases may explain the differences in inhibition by amino-1,2,4-triazole, which is known to react with compound I. The fact that the

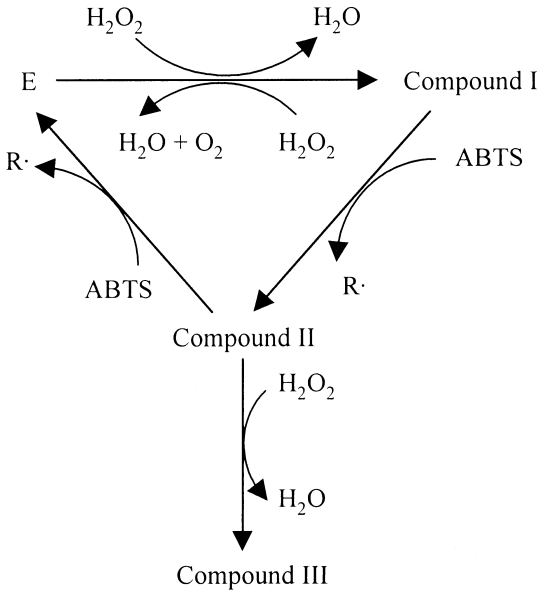

Fig. 7. Catalytic cycle of catalase-peroxidases

A. fulgidus catalase-peroxidase is inhibited by amino-1,2,4-triazole, unlike all other catalase-peroxidases, suggests that its catalytic cycle involves higher steady-state concentrations of compound I. It can be expected that in the presence of an electron donor such as ABTS, the steady-state concentration of compound I is lower than that when only H_2O_2 is present. This could explain the higher concentrations of amino-1,2,4-triazole, hydroxylamine, and sodium azide needed for 50% inhibition in the presence of ABTS. Cyanide inhibition required identical inhibitor concentrations, which is conceivable because cyanide, in contrast to the other inhibitor compounds, does not react with compound I, but with the native enzyme.

Unlike monofunctional catalases, the *Archaeoglobus* enzyme could be reduced by dithionite. Also the narrow pH optimum of the catalase and peroxidase activity found here is typical for catalase-peroxidases. The pH optimum of 4.5 for the peroxidase is the lowest reported for catalase-peroxidases. The other characteristics of the *Archaeoglobus* enzyme are typical for heme proteins in general or those of catalase-peroxidases in particular. The inhibition by azide, cyanide, and hydroxylamine is a common property of heme enzymes. The UV–visible spectral analysis indicated the presence of ferric heme (protoheme IX), which was confirmed by EPR spectroscopy. In addition, EPR of the nitrous oxide complex showed that the proximal ligand is a histidine, which could also be predicted from the sequence alignment. Based on the alignment, His-249 of the *A. fulgidus* sequence may act as the proximal ligand, and a conserved Trp-300 may interact with the imidazole ring of the histidine. On the distal side, three conserved residues, viz., His-87, Arg-83, and Trp-86, could form the ligand pocket for H_2O_2. Despite this conserved heme-binding site, only 0.25 heme was found per subunit. This low heme content also explains the low *RZ*-ratio of 0.32 (usually around 1 in typical catalases). The heterologous expression system used here may have resulted in an incomplete synthesis of the holoenzyme. However, similar low heme contents, ranging from 0.25 to 0.5, have been found for other catalase-peroxidases isolated from the original host. These findings may be explained by a partial loss of the heme during purification. It remains, however, peculiar that all catalase-peroxidases behave similarly in this respect. It has been suggested that the heme of catalase-peroxidases, in contrast to those of monofunctional catalases, is more easily accessible because it is located close to the surface of the protein (Hochman and Shemesh 1987). This accessibility might explain the relatively easy loss of the heme, and in addition it could also be the reason for the enzyme's ability to act as peroxidase.

Because *A. fulgidus* is a hyperthermophilic organism, the stability of the catalase-peroxidase was of interest. In the absence of H_2O_2, the enzyme indeed showed a high intrinsic stability. However, in the presence of even low H_2O_2 concentrations (1 mM), a half-life of only 60 s was found. There are two possible explanations for this inactivation, viz., (i) oxidative destruction of the porphyrin ring or (ii) formation of compound III. Porphyrin destruction is an irreversible process and results in the formation of verdoheme compounds. UV–visible spectroscopy of the inactivated enzyme, however, did not reveal such compounds. Formation of compound III is a reversible process and occurs when excess H_2O_2 is added to native enzyme. This compound is not involved in the normal reaction cycle, and, thus, formation of compound III results in an apparent inactivation. Compound III may be converted back to native enzyme via a one-electron oxidation by a radical cation. For example, ABTS radicals formed in the peroxidase reaction may provide such radical cations, and thus enable reactivation by the conversion of compound III to native enzyme. This reasoning may also apply to the *Archaeoglobus* enzyme, where H_2O_2 inactivation might have been caused by compound III formation, and the stabilizing effect of ABTS may then be explained by the conversion of compound III back to native enzyme.

The physiological function of catalase-peroxidases is the removal of H_2O_2, which is generated by the incomplete reduction of oxygen to water. Although *A. fulgidus* is assumed to be a strict anaerobe, occasional exposure to oxygen is conceivable in the marine environment (Prieur 1997). It is, therefore, likely that this organism possesses mechanisms that enable it to survive transient exposure to oxygen. Cell-free extracts of anaerobically grown *A. fulgidus* showed low (~1.4 U/mg) but significant catalase activity (Abreu et al. 2000). In addition to the catalase-peroxidase gene, several other genes involved in oxygen detoxification have been identified in the genome. For instance, neelaredoxin (Nlr) may form H_2O_2 by reduction or dismutation of superoxide (Abreu et al. 2000). On the other hand, H_2O_2 may also be formed by NADH oxidases. The *A. fulgidus* genome contains eight putative NADH oxidase genes, of which at least one is known to produce H_2O_2 (unpublished results). Further details on the role of the catalase-peroxidase in detoxification and the effect of exposure to oxygen on enzyme levels is currently being investigated.

Acknowledgments This work was funded by the European Community under the Industrial & Materials Technologies Programme (Brite-Euram III) (Contract BRPR-CT97-0484).

References

Abreu IA, Saraiva LM, Carita J, Huber H, Stetter KO, Cabelli D, Teixeira M (2000) Oxygen detoxification in the strict anaerobic archaeon *Archaeoglobus fulgidus*: superoxide scavenging by Neelaredoxin. Mol Microbiol 38:322–334

Bradford MM (1976) A rapid and sensitive method for the quantification of microgram quantities of protein utilizing the principle of protein-dye binding. Anal Biochem 72:248–254

Brown-Peterson NJ, Salin ML (1993) Purification of a catalase-peroxidase from *Halobacterium halobium*: characterization of some unique properties of the halophilic enzyme. J Bacteriol 175:4197–4202

Cendrin F, Jouve HM, Gaillard J, Thibault P, Zaccai G (1994) Purification and properties of a halophilic catalase-peroxidase from *Haloarcula marismortui*. Biochim Biophys Acta 1209:1–9

Fraaije MW, Roubroeks H, Hagen WR, van Berkel WJH (1996) Purification and characterization of an intracellular catalase-peroxidase from *Penicillium simplicissimum*. Eur J Biochem 235:192–198

Hagen WR (1981) Dislocation strain broadening as a source of anisotropic line width and asymmetrical line shape in the electron paramagnetic resonance spectrum of metalloproteins and related systems. J Magn Reson 44:447–469

Hartzell CR, Beinert H (1974) Components of cytochrome *c* oxidase detectable by EPR spectroscopy. Biochim Biophys Acta 368:318–338

Hochman A, Shemesh A (1987) Purification and characterization of a catalase-peroxidase from the photosynthetic bacterium *Rhodopseudomonas capsulata*. J Biol Chem 262:6871–6876

Jaenicke R (1991) Protein stability and molecular adaptation to extreme conditions. Eur J Biochem 202:715–728

Klenk HP, Clayton RA, Tomb JF, White O, Nelson KE, Ketchum KA, Dodson RJ, Gwinn M, Hickey EK, Peterson JD, Richardson DL, Kerlavage AR, Graham DE, Kyrpides NC, Fleischmann RD, Quackenbush J, Lee NH, Sutton GG, Gill S, Kirkness EF, Dougherty BA, McKenney K, Adams MD, Loftus B, Peterson S, Reich CI, McNeil LK, Badger JH, Glodek A, Zhou LX, Overbeek R, Gocayne JD, Weidman JF, McDonald L, Utterback T, Cotton MD, Spriggs T, Artiach P, Kaine BP, Sykes SM, Sadow PW, KP D'Andrea, Bowman C, Fujii C, Garland SA, Mason TM, Olsen GJ, Fraser CM, Smith HO,

Woese CR, Venter JC (1997) The complete genome sequence of the hyperthermophilic, sulphate-reducing archaeon *Archaeoglobus fulgidus*. Nature 390:364–370

Laemmli UK (1970) Cleavage of structural proteins during the assembly of the head of bacteriophage T4. Nature 227:680–685

Leuschner C, Antranikian G (1995) Heat-stable enzymes from extremely thermophilic and hyperthermophilic microorganisms. World J Microbiol Biotechnol 11:95–114

Levy E, Eyal Z, Hochman Z (1992) Purification and characterization of a catalase-peroxidase from the fungus *Septoria tritici*. Arch Biochem Biophys 296:321–327

Loprasert S, Negoro S, Okada H (1988) Thermostable peroxidase from *Bacillus stearothermophilus*. J Gen Microbiol 134:1971–1976

Loprasert S, Negoro S, Okada H (1989) Cloning, nucleotide sequence, and expression in *Escherichia coli* of the *Bacillus stearothermophilus* peroxidase gene (*perA*). J Bacteriol 171:4871–4875

Marcinkeviciene JA, Magliozzo RS, Blanchard JS (1995) Purification and characterization of the *Mycobacterium smegmatis* catalase-peroxidase involved in isoniazid activation. J Biol Chem 270:22290–22295

Morris SL, Nair J, Rouse DA (1992) The catalase-peroxidase of *Mycobacterium intracellulare*: nucleotide sequence analysis and expression in *Escherichia coli*. J Gen Microbiol 138:2363–2370

Mutsuda M, Ishikawa T, Takeda T, Shigeoka S (1996) The catalase-peroxidase of *Synechococcus* PCC 7942: purification, nucleotide sequence analysis and expression in *Escherichia coli*. Biochem J 316:251–257

Nadler V, Goldberg I, Hochman A (1986) Comparative study of bacterial catalases. Biochim Biophys Acta 882:234–241

Obinger C, Regelsberger G, Strasser G, Burner U, Peschek GA (1997) Purification and characterization of a homodimeric catalase-peroxidase from the cyanobacterium *Anacystis nidulans*. Biochem Biophys Res Commun 235:545–552

Pierik AJ, Hagen WR (1991) S=9/2 EPR signals are evidence against coupling between the siroheme and the Fe/S cluster prosthetic groups in *Desulfovibrio vulgaris* (Hildenborough) dissimilatory sulfite reductase. Eur J Biochem 195:505–516

Prieur D (1997) Microbiology of deep-sea hydrothermal vents. Trends Biotechnol 15:242–244

Regelsberger G, Obinger C, Zoder R, Altmann F, Peschek GA (1999) Purification and characterization of a hydroperoxidase from the cyanobacterium *Synechocystis* PCC 6803: identification of its gene by peptide mass using matrix assisted laser desorption ionization time-of-flight mass spectrometry. FEMS Microbiol Lett 170:1–12

Sambrook J, Fritsch EF, Maniatis T (1989) Molecular cloning: a laboratory manual, 2nd ed. Cold Spring Harbor Laboratory Press, Cold Spring Harbor, NY

Schumacher W, Holliger C, Zehnder AJB, Hagen WR (1997) Redox chemistry of cobalamin and iron–sulfur cofactors in the tetrachloroethene reductase of *Dehalobacter restrictus*. FEBS Lett 409:421–425

Stetter KO (1988) *Archaeoglobus fulgidus* gen. nov., sp. nov.: a new taxon of extremely thermophilic archaebacteria. Syst Appl Microbiol 10:172–172

Triggs-Raine BL, Doble BW, Mulvey MR, Sorby PA, Loewen PC (1988) Nucleotide sequence of *kat*G, encoding catalase HPI of *Escherichia coli*. J Bacteriol 170:4415–4419

Welinder KG (1991) Bacterial catalase-peroxidases are gene duplicated members of the plant peroxidase superfamily. Biochim Biophys Acta 1080:215–220

Welinder KG (1992) Superfamily of plant, fungal and bacterial peroxidases. Curr Opin Struct Biol 2:388–393

Yonetani T, Yamamoto H, Erman JE, Leigh JS, Reed GH (1972) Electromagnetic properties of hemoproteins. J Biol Chem 247: 2447–2455